The 17th International Conference on Space Operations

Safety and Sustainability of Space Missions (SSU)
Post-Anomaly Analysis for Space Weather Events

Locating and Stopping Orbital Debris

Paul Iustin Vartolomei[a]*

[a]"Andrei Saguna" National College, Șirul Andrei Șaguna Nr. 1 Street, Brasov City, Brasov County, Romania 500123

ARTICLE INFO

Keywords:

Orbit
Collision
Orbital Debris
Trajectory
Velocity

ABSTRACT

The abundance of orbital debris in the Low Earth Orbit, Geosynchronous Orbit and transit orbits represents an increased risk of collision for missions that are to come. Since tracking and observing smaller, individual orbital debris has proven to be a challenge even for the most advanced Earth-based observatories, addressing this issue would benefit the welfare of current spacecraft and the safety of future missions.

The proposed concept for reducing said risk consists of two stages: detecting the velocity and position vectors of orbital debris, thus estimating their trajectory, by a ring-like spacecraft, having in its interior three separate infrared proximity sensor arrays, afterwards intentionally colliding them with an impact-resistant material, transported and aligned to the previously identified orbit by another ring-like spacecraft. Initially, each proximity sensor array serves to obtain the precise position of the debris at a certain point, and using the time interval between two successive detections, the instantaneous velocity and its orientation can be easily calculated. These parameters alone can determine the inclination and semi-major axis of the debris' orbit and using computer simulations that take into account multiple eccentricities and three-body effects, a curve can be approximated. Consequently, a signal triggers the additional spacecraft to align with the debris' trajectory, reducing its speed or stopping it entirely after the collision. This innovative concept provides a line of defence against small orbital debris and can prove to dramatically reduce their number.

Corresponding Author:

Paul Iustin Vartolomei,
"Andrei Saguna" National College,
Brasov, Romania.
Email: paul.iustin2005@gmail.com

1. INTRODUCTION

The growing number of orbital debris poses a great obstacle to the progress of humanity's space exploration process due to the imminent risk of collisions that can be considered a safety hazard for future space missions. Not only do the affected spacecraft experience a decrease in performance, or at worst, cease to function, they also may contribute to the proliferation of these unwanted objects. This phenomenon, more known as the Kessler Syndrome [1], initially studied by NASA scientist Donald J. Kessler in 1978, proposes that once a certain object density has been reached in the Low Earth Orbit, and by extension, any crowded orbit, the aforementioned objects could initiate a cascade of collisions, which would make said orbit uninhabitable for future spacecraft.

The proposed solution for this devastating calamity would be eliminating excess bodies from each of those orbits in order to decrease their density. However, the problem with this solution is the sheer number of objects that populate these regions. Studies show how it evolved, ever since the dawn of the Space Race, when the first satellite was launched. They are expected to increase in number, as the trend shows, so a development in the technology of orbital debris removal is needed. This study proposes utilizing remote, robotic spacecraft in order to contribute to cataloging and effectively removing debris.

Since many objects with radiuses of more than 1mm can be tracked from ground observatories, this study focuses on slightly smaller sizes, considering that their abundance and almost unpredictable movement can inflict significant damage to human progress.

2. METHODS

2.1 Description

The proposed concept for this operation consists of two main parts: detection (or spotting) and removal (stopping) of the space debris. The Spotters are tasked to identify the

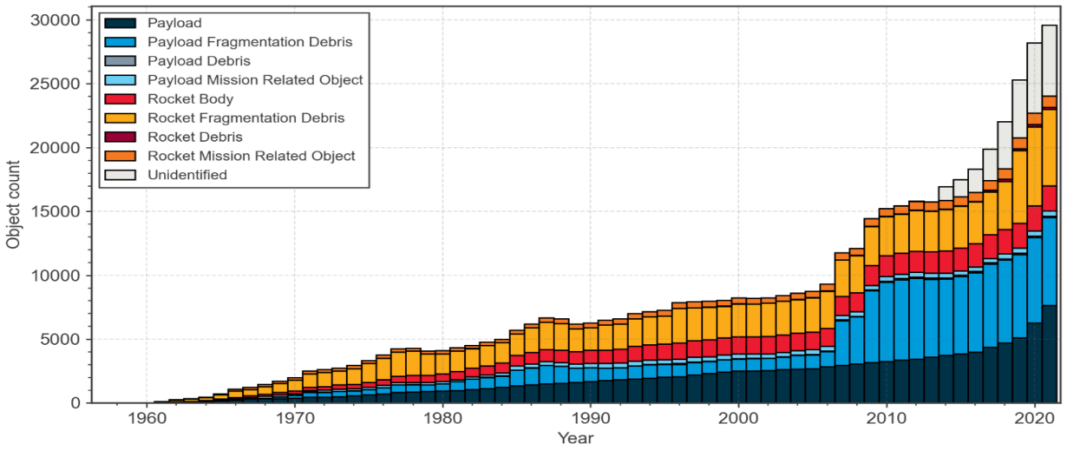

Fig. 1. Evolution of the number of space debris (courtesy of ESA)

velocity and position vectors of the debris once they pass through them, data that would further be transmitted and used by the orbital determination algorithm in a ground station (preferably placed on the surface of the Moon). Once computed, the coordinates of the desired spot will then be sent forward to The Stoppers, which will place themselves there in order to collide with the debris. Note that due to the conveniently small period of the debris orbiting at lower altitudes, the Stoppers would not be required to travel long distances in a short time. Once the collision is confirmed, the cycle will be repeated.

2.2 Anatomy of a Spotter

For the Spotter to correctly identify the size and position of the debris it detects, the array of infrared sensors must be positioned in such a fashion that it would have almost no blind-spots (the entire interior area must be covered by the sensors). In that case, a torus shape would be very inconvenient due to the intersection of rays at the center and lower coverage at the margin.

Thereby, the spotter was projected as a rectangular frame, with three planes of arrays. The sensors have been arranged so that a ray emitted by a module wouldn't be received by the module at the other end, but reflected back to the first one.

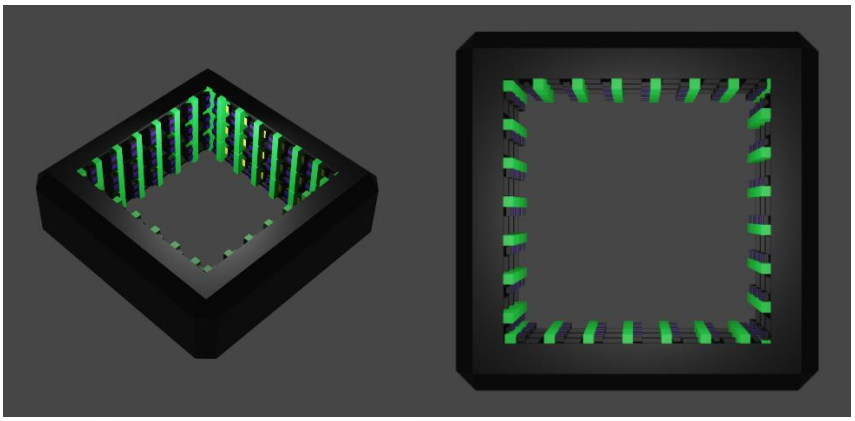

Fig. 2. Side- and Top-view of the frame of a small Spotter. The proportions of the overall build are accurate; however, the LED/board ratio of 3/1 has been modified to 1/1 for render purposes. Given the dimensions, the frame has an interior side length of 56mm, exterior side length of 73.6mm and height of 34.6mm. Each array has 28 sensors (7 on each side). The size of the actual model may vary given that the spacecraft is scalable.

To assure maximum coverage, the gap between two successive sensors must be increasingly smaller. In the proposed 3D small model for the Spotter (Fig. 2.), said gap is around 4mm, given the size of the infrared sensor (the used model was a POLOLU 38kHz analogue IR proximity sensor with a height of 5.02mm, receiver LED height of 3mm and emitter height of 1mm), which aims to reduce blind-spots while maintaining the accuracy of the radius determination process.

The three arrays have a height difference of 1mm between two adjacent sensors, which implies a 1.7 mm difference between two separate receivers, which will act as the "Δz" distance in the detection algorithm.

The sensors are connected through ADC pins to three ESP32 boards located inside the frame, but not in the main bus (84 total sensors and 28 sensors/board), and use pin interrupts to signal the presence and the position of any object that may be detected. They send the information to a Raspberry Pi Zero 2 W board at the heart of the spacecraft bus. The RPI is tasked with calculating the x, y and z components of both velocity and position vectors and forwarding these values via an antenna.

As for the spacecraft bus itself, it is equipped with two 9V rechargeable batteries (which power the sensor arrays and the instruments respectively), the RPI Zero 2 W, an antenna, a receiver and a gyroscope (for receiving its own position and calculating its orientation relative to Earth. For the small model of the Spotter, propulsion via thrusters for orbit correction and attitude control would be unwise due to its size and weight, since orbital decay won't pose a problem for shorter service periods.

The mass of the small model of the Spotter can be calculated with the help of proportions and considering graphene as the frame material. Calculation returns a mass of roughly 466 grams, also taking into account the mass of the other instruments. The center of mass of the Spotter will be located somewhere near the spacecraft bus, mainly due to the batteries and the other important instruments.

While searching for debris, the Spotter will be charged by solar panels integrated in the frame and connected to the batteries.

2.3 Anatomy of a Stopper

As the Spotter must identify the orbits of the debris, the Stopper is tasked to essentially remove them from the equation. The principle used is quite simple and relatively common. So far, it has been applied to tethered plate satellites, that can sweep debris as they encounter them (Takeichi et al, 2021) [2], or direct collisions with the solar panels of other satellites, however the Stoppers are provided with precise coordinates and instructions, which guarantee the removal of a considerable number of orbital debris.

Instead of a solar panel or a tethered plate, the Stopper frame encloses a thick layer of graphene in its interior that will collide with the space debris at a predetermined time and place.

Since the Stopper is large enough to be equipped with means of transportation, it also helps to deploy Spotters in various orbits for achieving maximum efficiency and coordination. The frame of a Stopper is similar to its counterpart, however on a much larger scale.

In the process of designing the spacecraft, the key aspects for determining both its size and mass were the thrusters, more precisely, two Hall effect ion thrusters that use Krypton as fuel, placed parallel to each other at to opposite ends of the frame. For navigation, the thrusters can be maneuvered via servomotors that alter their orientation. They are aligned with the weight center of the spacecraft. They generate 83mn at 1.35kW and with a specific impulse of 1300 s, while having a mass of 3.5 kg and a specific length of 15cm [3].

As for stopping the debris, the role of the tethered plate is played by a replaceable layer of graphene, with a thickness of around 20cm and length of 75cm, to account for inaccuracies in the detection algorithm. It is contained by the outer frame.

The spacecraft bus is located in the upper compartment of the Stopper, and it consists of several instruments, such as the antenna and receiver, whose purpose is to allow the communication between the ground base and the stopper and the main processing unit, tasked with interpreting the received coordinates and relocating to the proper position.

The lower compartment stores the battery (a 112 Ah, 29.6 V battery with a mass of 28kg) and the spotter storage. The required 0.6L of Krypton are stored inside the frame. The mass of the Stopper is approximately 527.5kg.

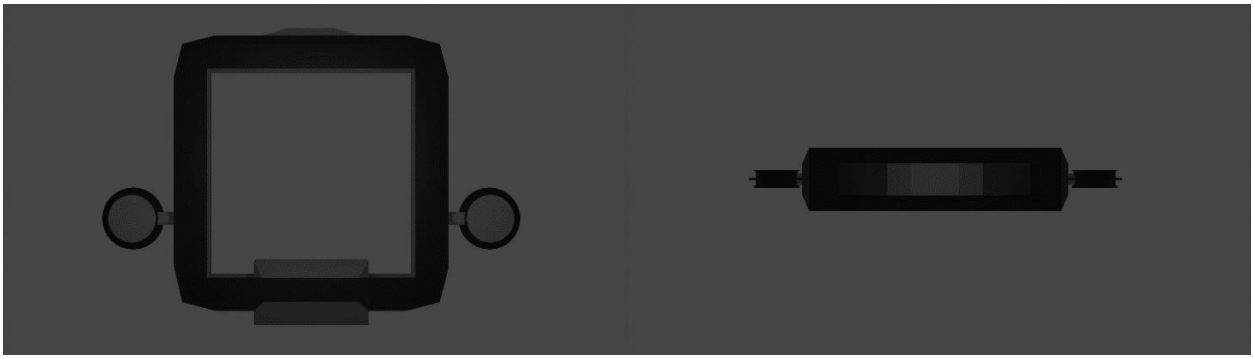

Fig. 3. Front- and top-view of the Stopper. Similarly to its counterpart, the proportions are accurate and the model is scalable. The proposed build has an exterior length of 100cm, interior length of 75cm and thickness of 20cm. The specific length of the thrusters is 15cm.

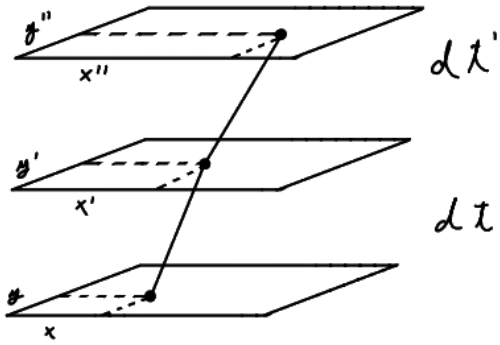

Fig. 4. A visual representation of the determination algorithm's principles. In the time intervals specified at the side, the detected body shifts between two separate point in the detection planes

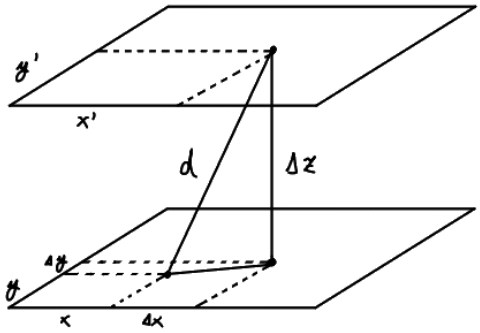

Fig. 5. The measured changes, Δx, Δy and Δz, can be used to compute the distance traveled by the detected body in the specified time interval, thus making the calculation of the velocity possible.

2.4 Debris Detection Algorithm

The concept used for debris detection slightly resembles that of a radar. The infrared sensors are essentially made up of an emitter and a receiver. The emitter radiates rays of light in a somewhat continuous fashion, and the receiver detects those rays once they have been reflected by an arbitrary body. Based on the time interval between emission and detection, and taking into account the constancy of the speed of light, such a sensor can "compute" the distance between itself and that arbitrary body.

The advantage of this type of sensor is that the detection is arguably instantaneous, compared to an ultrasonic proximity sensor, which uses sound waves that have a way lower velocity and that are unusable at high altitudes due to a less dense atmosphere.

The Spotters have three layers of sensor arrays, which act as independent detection planes (Fig 4). Once a debris, or any body for that matter, enters the plane of the first array, its presence is recorded by at least two different proximity sensors: one for calculating the "x" coordinate and one for the "y" coordinate; effectively pinpointing the precise location of the body relative to the bottom-left corner of the Spotter.

This procedure is analogous for the other two layers. However, the point of having multiple arrays is to detect not only the body's position, but also the modification of its position with respect to time.

The program onboard the RPI is tasked to record the time elapsed between two successive detections (i.e., the time it takes for said body to move between the first and second layer, or second and third layer of sensors). Consequently, given that the distance between two detection points is known, the instantaneous velocity of the body can be calculated (Fig 5.). Not only that, but having the option of recording two values for the instantaneous velocity, the ground station will be able to compute two separate trajectories, which greatly benefits the accuracy of orbit determination.

This algorithm is conceived as a sequence of events, which can detect up to two bodies at once (thanks to the facilities of the ESP32 boards, however the explanation will detail the case of only a single body). The sequence commences the instant the first layer returns a set of coordinates. The coordinates are then transmitted and stored inside of the RPI, which automatically starts a chronometer, while the first array stops the search for objects. After the second set of coordinates is returned, the chronometer stops and the time elapsed is stored and used to compute the first velocity. The second time interval starts being recorded, as the second array stops searching. Finally, once the third set of coordinates is returned, the chronometer stops again and then both velocities can be computed.

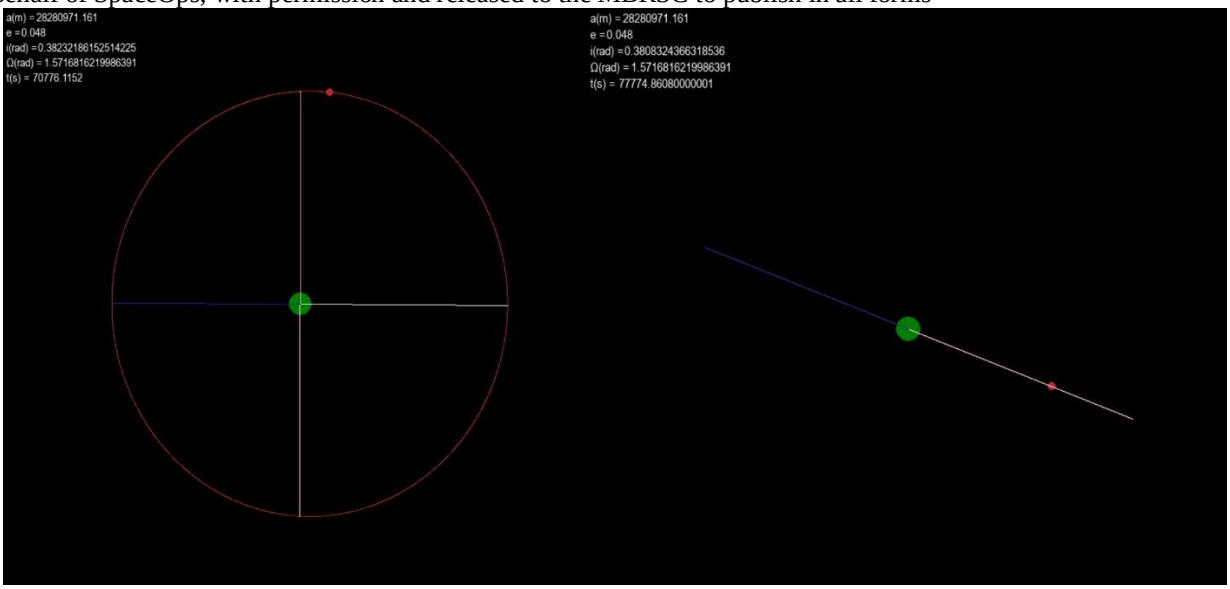

Fig. 6. The illustration of a debris' orbit returned by the simulation. The image on the left represents the trajectory as seen from the top of the Moon's orbital plane and the image on the right is the orbit viewed from an observer inside the Moon's orbital plane. The top-left corner of each image contains important orbital parameters, such as the pseudo- semi-major axis and eccentricity, the longitude of the ascending node and the elapsed time.

The first array may once again start searching for bodies. Note that in order for the higher order arrays to start searching for bodies, they need a confirmation from the previous arrays, so that errors and confusions are avoided (i.e. if the first array detects an object, and by coincidence, the third array detects something else just before the second does, said detection isn't recorded).

As for the determination of the position vector, the algorithm will make use of both the coordinates of the detected body relative to the Spotter and the coordinates of the spacecraft relative to the Earth. As mentioned before, the Spotter is equipped with all the necessary instruments to handle this task accurately as well.

Lastly, the final important variable that can be obtained from the Spotter is the diameter of the observed object. Depending on the number of triggered sensors and taking into account their height of 5,02mm, each array can individually compute a certain diameter, given the frame's interior length of 56mm. At the end of the detection sequence, the final result will be the average of the three returned values (one value/array).

2.5 Orbital determination algorithm

After the position and velocity vectors have been identified (the mean Cartesian coordinates for position and two sets of x, y and z values for the velocity) and transmitted to a ground station, orbital determination can commence.

The program [4] used to simulate and predict the orbit of an arbitrary space debris is based on a version of "Simulating Planetary Orbits" (Kuchling et al, 2011) [5]. However, it has been heavily augmented to suit the needs of this study.

The input variables are the position of the Moon, along with the position and velocity vectors of the debris, the debris' radius and its approximate mass.

To stay consistent with the real motion of bodies in such conditions, the simulation has been updated to take into account other forces that act on the debris, such as atmospheric drag, solar radiation pressure and third body perturbations. Not to mention, the simulation computes the motion of debris in a three-dimensional space, using the Moon's orbit as the reference frame for calculating other orbital parameters.

The atmospheric drag [6] was computed with the help of the relationship between temperature, pressure and density, while considering that the simulated body is spherical (which in turn gives a drag coefficient of ½).

$$F_D = C_D \frac{\rho v^2}{2} A$$

All of the other variables are known quantities that will have been calculated by the detection algorithm.

In the case of Solar radiation pressure, which takes its toll on various parameters of the body's orbit (S. O. Belkin et al, 2021)[7],

$$P = \frac{I_f}{c} cos^2\alpha$$

the value of the solar irradiance I_f is known (since the distance from the Sun is around 1 AU) and the incident angle is always zero, which in turn gives

$$F_{rad} = \frac{I_f}{c}\pi r^2.$$

Naturally, the algorithm takes solar radiation pressure into account only when the Sun isn't eclipsed by either the Earth or the Moon.

Applying third body perturbations from the Moon has already been accounted for in the initial cited simulation.

Along with the most relevant data, such as the array of points that represent the body's orbit, the code also computes the most basic orbital parameters, such as the semi major axis, eccentricity, inclination of the orbit and the longitude of the ascending node. This serves to catalogue debris that couldn't be removed for various reasons.

The same program has been used for simulating the debris' trajectory that will further be analyzed here. Since the orbit isn't quite a perfect ellipse, due to aforementioned external forces acting, it is relatively difficult to characterize it by using a single parameter.

However, this study uses the approximate eccentricity (or pseudo-eccentricity) of an ellipse with perigee and apogee values that coincide with the minimal and maximal distances between the debris and the Earth as a reference.

The variation of said eccentricity could identify how stable the orbit is and detail the overall impact of external forces on the debris' trajectory.

As the simulated debris orbits the Earth, the program tracks its overall distance from the center. If it is smaller than the previous value for the pseudo-perigee, the perigee is relocated to that certain point. The procedure is analogous for the apogee, but in this case, it resets only if the distance is larger than the previous apogee value. This, in turn, causes the "major axis" components to slightly shift over time. So, another parameter that will be more thoroughly investigated is the variation of their orientation.

3. Results and Discussions

3.1 Orbital Stability

3.1.1 Pseudo-Eccentricity

After simulating the proposed trajectory, with the initial values shown in the table below, the first studied stability-related parameter was the pseudo-eccentricity. Its variation with respect to time shows the tendency of the perigee's value to decrease or increase. That ultimately determines the fate of the debris, since once the perigee is low enough, the atmospheric drag may capture the debris in a graveyard-like orbit.

On the other hand, if the eccentricity is constant, the perigee also remains constant, which implies a stable orbit and a significant increase in the debris' lifetime. A decrease of the pseudo-eccentricity is highly unlikely, so this study will focus on the implications of the other cases.

Initial values	Debris Position (m)	Debris Velocity (m/s)	Moon Position (m)
x component	0	0	0
y component	25000000	3938.88	-384000000
z component	10000000	0	0

Table 1. The positional values for the simulated debris. It is considered to be a spherical body with a radius of 1mm and a mass of 0.0113g (using aluminum's density of 2.71g/cm^3).

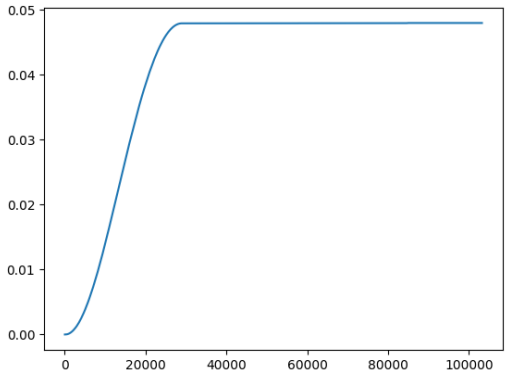

Fig. 7. Pseudo-eccentricity with respect to time.

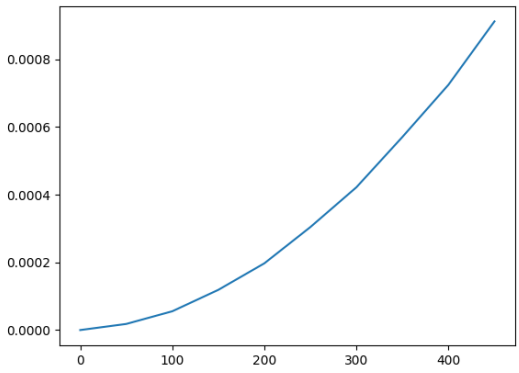

Fig. 8. The variation of the Pseudo-eccentricity with respect to the variation of the detected velocity.

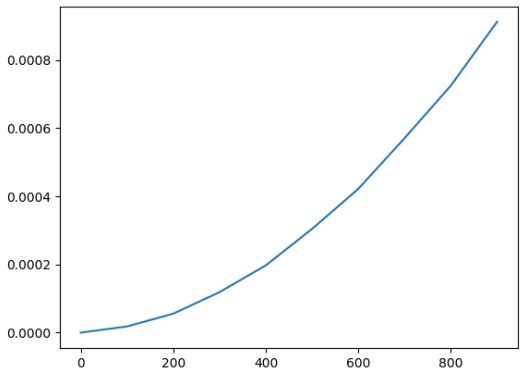

Fig. 9. Similar to fig. 8., but on a broader range.

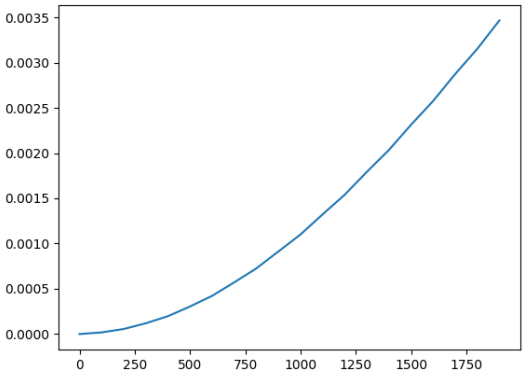

Fig. 10. Significant increase in pseudo-eccentricity is detected only at higher velocity differences

Figure 7 showcases the behavior of the pseudo-eccentricity with respect to time. The initial increase is due to the fact that a permanent apogee hadn't been selected yet (until the timestamp of around 30000 seconds, the distance between the Earth and the debris grew continuously, which accounts for said increase). From that point on, however, the value of the eccentricity remained relatively constant, which implies that the proposed orbit is stable. The small variations determined by external forces are visibly insignificant, which implies that, at those coordinates, relying on drag or radiation pressure to remove debris is unwise (their impact on pseudo-eccentricity is almost unnoticeable in the long term).

Figures 8, 9 and 10 display the variation of the pseudo-eccentricity with respect to the variation of the detected velocity. The purpose of this measurement is to take into account errors in the detection algorithm and to assure the removal of the debris without damaging the Stopper's frame. In the case of the proposed trajectory, the difference between two pseudo-eccentricities begins to become noticeable only at larger velocity variations, which implies that small errors in the detection algorithm won't have a large impact, especially if the Stopper will act close to the detection point. Besides, these graphs also show how fragile the stability of the orbit is (i.e. the impact that modifying the velocity of the body has on its orbit).

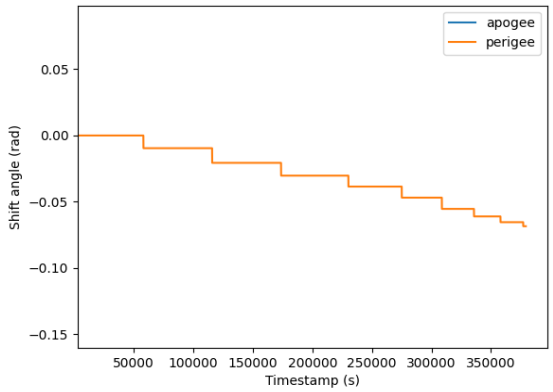

Fig. 11. The pseudo-perigee's shift

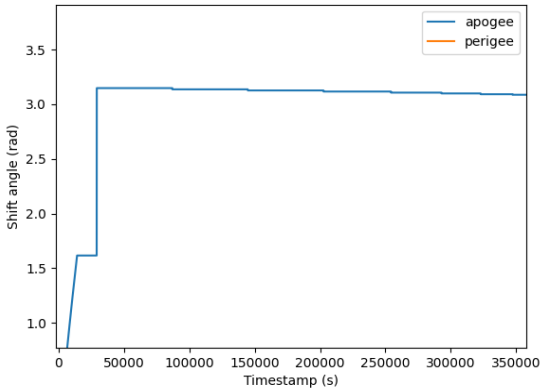

Fig. 12. The pseudo-apogee's shift

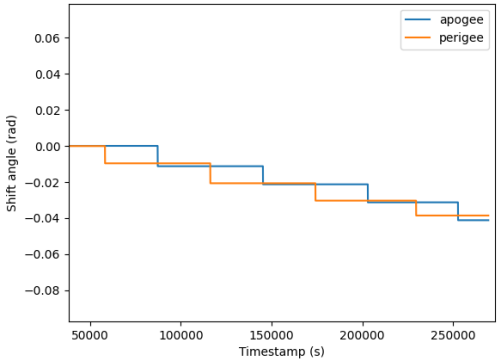

Fig. 13. The overall orbital shift with respect to time. The apogee has a higher shift tendency.

3.1.2 Orientation of the Semi-major Axis components

The other factor that characterizes the orbit's stability is the shift of the apogee and perigee respectively. This happens because of the slight decrease in pseudo-eccentricity caused by the external forces and determines a shift of the overall trajectory. If it would remain ignored, it could lead to significant errors in the orbital detection algorithm and possibly Stopper damage. The shift is measured in radians.

Figure 11 displays the behavior of the perigee axis with respect to time for the proposed trajectory. In this case, the perigee shifts "backwards" (the opposite direction of the body's rotation). This means that after a complete orbit, the minimal distance is always reached before the previous perigee. It also confirms the constant decrease of the perigee value (another interpretation of the results from the analysis of the pseudo-eccentricity in subchapter 3.1.1).

Figure 12 shows the apogee's shift, which behaves similarly to the one of the perigee's. However, in this case, the maximal distance is reached before the previous apogee. The apogee initially experiences an abrupt increase in shift until the 30000s timestamp because of reasons stated previously (the continuous growth of the distance between the Earth and the debris). However, to get to a firm conclusion about the orbit's stability from this point of view, a direct comparison between these shifts is required.

After some offsets to account for the apogee's growth (around π rad to be precise),

Figure 13 displays the angular motion of the entire semi-major axis. This confirms the fact that the entire orbit has a tendency to shift backwards, and that even though the orbit seems stable from a pseudo-eccentricity point of view, it actually is continuously and visibly affected by the external forces acting on the debris.

3.2 Coverage and utility

The aim of this study is to effectively tackle the problem of the current excessive number of orbital debris. Given all the information about the methodology, the next step would be to actually see the potential of the proposed operation and the quantity of debris it can actually catalogue and remove. Evidently, this directly depends on the active number of Stoppers and Spotters, and on their altitude (or the debris density at that certain altitude).

The number of removed debris is equivalent with the number of debris that pass through the Spotter. This means that it actually resembles the hypothetical number of debris collisions with the interior of the frame, if it were a solid. With the help of the methodology from S. Le May et al. 2018 [8], this number can be quantified. The coverage of a single Spotter has been determined to be 3,136mm^2, which acts as the cross-section area A_c. Therefore, the collision number can be written as:

$$N_{col} = \sum_{i=1}^{n} F_i * A_c * T$$

, where F_i is the flux of orbital debris for a given Spotter, T is the operational lifetime of the spotter, and n is the total number of Spotters.

The only factor that is critical for determining the collision number is the spatial density of the debris at a given altitude, since both the operational time and number of Spotters can be controlled. In that regard, while calculating this number the distribution of debris will be considered uniform, and the spatial density of these bodies will be their number divided by the volume in which the Spotters will be active. Given the small size of these Spotters, they are very easy to manufacture and deploy, so their number can reach the hundreds or even thousands.

The operational lifetime of an individual spotter is relatively hard to estimate, however as a whole, the operation can be expected to last for years.

Since the number of space debris is expected to rise significantly in the future, especially in the LEO, the number of collisions will be written as a function of the overall debris number in the covered region.

3.2.1 The Spotter's Orbit

Near-circular debris orbits cause them to have an overall constant velocity, specific to their orbital radius. This in turn implies that it would be unwise for the Spotter to also have a circular orbit since it would detect significantly less debris (the relative velocity of the debris with respect to the Spotter would be very low, causing a reduced debris flux). This is why, after being deployed by its larger counterpart, the Spotter will be injected into an orbit with a higher eccentricity, with perigee and apogee values ranging from the lower and upper bounds of regions with a high debris density.

By choosing an elliptical orbit, the spotter will be able to cover more "debris orbits", increasing the probability of detection and the debris flux. Also, launching a higher number of spotters in orbit and distributing them so that their respective major axes would be slightly tilted will greatly help the removal of debris and contribute to the purpose of the operation.

However, proceeding this way would increase the difficulty of calculating the debris flux. Since the Spotter's velocity won't have the same orientation as the debris' velocity and the distance from the Earth to the Spotter will continuously vary, this would also mean that the flux won't remain constant. Thereby a thorough examination of the variation of said flux is required.

Using data from Colombo, et al. 2016 [9], the upper bound of the coverage region is placed at an altitude of around 1600km and the lower bound at 600km. This implies a semi-major axis of around 1100km, an orbital period of 36.6h and an eccentricity of 0.45 for the Spotter's orbit. Further, the vis-viva equation can determine the velocity of the Spotter at any

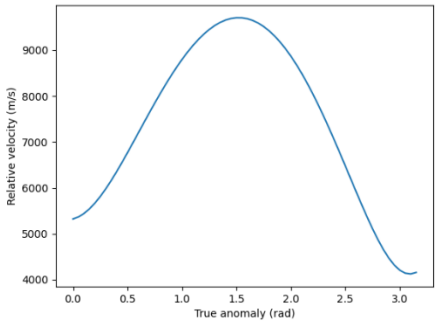

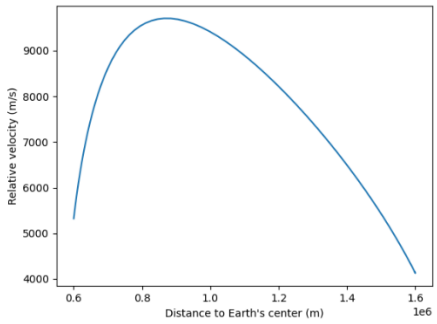

Fig. 14. and 15. The relative velocity of debris traveling in the same direction as the Spotter, with respect to its true anomaly and distance from Earth.

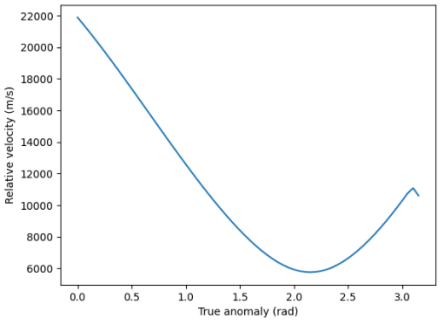

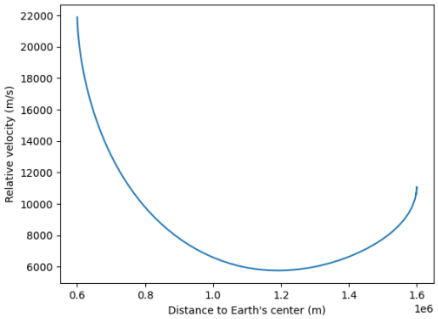

Fig. 16. and 17. The relative velocity of debris traveling in the opposite direction, with respect to its true anomaly and distance from Earth.

given point of the orbit, knowing the distance between it and the Earth.

$$v = \sqrt{G * M\,(\frac{2}{r} - \frac{1}{a})}$$

That distance also serves as an important parameter in calculating the debris' velocity, assuming they have near-circular orbits.
The angle between the direction of the two velocity vectors can be computed with the help of the angular momentum conservation of the Spotter

$$\sin\beta = \frac{a}{r}\sqrt{\frac{(1-e^2)r}{2a-r}}$$

, and taking into account the fact that the debris' velocity always makes a 90-degree angle with its position vector when travelling in the same direction as the Spotter, or 270 degrees when travelling in the opposite direction.

Figures 14 – 17 showcase the behavior of the Relative velocity of the debris with respect to the true anomaly of the Spotter and the distance from Earth. For the first set of plots, the relative velocity peaks around π/2, and lowers as the Spotter approaches the apogee and perigee respectively (the two points in the orbit where the angle between the velocity vectors is zero. The second set of plots shows, as expected an

increase in relative velocity near the extremities of the orbit.

After running the simulation and inputting the results into the previously mentioned formula, the number of space debris detected by a single spotter during one orbital period is $1.43 * 10^{-11}$ N, where N is the total number of space debris located at altitudes between 600 and 1600km.

4. Summary and Conclusions

This study proposed an efficient and effective way to deal with the increasing number of space debris, while also keeping track of and analyzing their trajectories to help prevent future collisions, understand their behavior and stop the proliferation of these unwanted bodies.

Both the Spotters and the Stoppers are scalable models and their dimensions can be altered, however, the proposed sizes are more efficient for identifying debris with slightly smaller radii.

The debris detection algorithm can precisely determine the position and velocity vectors of up to two debris at the same time, along with their approximate diameter and mass, considering that the majority of these smaller bodies consist of aluminum or paint.

The orbital determination algorithm serves to estimate the trajectory of any identified debris, and select a proper place for the Stopper, where it can collide with the body and effectively mitigate it. It also investigates other important orbital parameters for collision prevention and cataloging purposes. The stability of the orbit is also analyzed, aspect that could determine the priority for removal of the debris.

References

[1] D.J. Kessler, Collisional cascading: the limits of population growth in low Earth orbit, Adv. Space Res. ll (12) (1991) 3–6.

[2] Noboru Takeichi, Naoki Tachibana, A tethered plate satellite as a sweeper of small space debris, Acta Astronautica, Volume 189, 2021, Pages 429-436, ISSN 0094-5765, https://doi.org/10.1016/j.actaastro.2021.08.051

[3] Michael Keidar, Isak I. Beilis, Chapter 4 - Plasma Dynamics, Editor(s): Michael Keidar, Isak I. Beilis, Plasma Engineering, Academic Press, 2013, Pages 127-171, ISBN 9780123859778, https://doi.org/10.1016/B978-0-12-385977-8.00004-4.

[4] Paul Iustin Vartolomei (2023) debris_trajectory [Source code] https://github.com/PaulDrt41/debris_trajectory.git

[5] Simulating Planetary Orbits – 50 Examples 1.0 documentation https://fiftyexamples.readthedocs.io/en/latest/gravity.html

[6] Kiyona Miyamoto, Toshihiro Chujo, Kei Watanabe, Saburo Matunaga, Attitude dynamics of satellites with variable shape mechanisms using atmospheric drag torque and gravity gradient torque, Acta Astronautica, Volume 202, 2023, Pages 625-636, ISSN 0094-5765, https://doi.org/10.1016/j.actaastro.2022.11.014.

[7]S.O. Belkin, E.D. Kuznetsov,
Orbital flips due to solar radiation pressure for space debris in near-circular orbits,
Acta Astronautica,
Volume 178,
2021,
Pages 360-369,
ISSN 0094-5765,
https://doi.org/10.1016/j.actaastro.2020.09.025.
[8] S. Le May, S. Gehly, B.A. Carter, S. Flegel,
Space debris collision probability analysis for proposed global broadband constellations,
Acta Astronautica,
Volume 151,
2018,
Pages 445-455,
ISSN 0094-5765,
https://doi.org/10.1016/j.actaastro.2018.06.036.
[9] COLOMBO, Camilla, et al. Spatial density approach for modelling of the space debris population. In: *26th AAS/AIAA Space Flight Mechanics Meeting*. 2016. p. 2749-2761.